ADVANCED MATERIALS
www.advmat.de

How Reproducible is the Synthesis of Zr–Porphyrin Metal–Organic Frameworks? An Interlaboratory Study

Hanna L. B. Boström, Sebastian Emmerling, Fabian Heck, Charlotte Koschnick, Andrew J. Jones, Matthew J. Cliffe, Rawan Al Natour, Mickaële Bonneau, Vincent Guillerm, Osama Shekhah, Mohamed Eddaoudi, Javier Lopez-Cabrelles, Shuhei Furukawa, María Romero-Angel, Carlos Martí-Gastaldo, Minliang Yan, Amanda J. Morris, Ignacio Romero-Muñiz, Ying Xiong, Ana E. Platero-Prats, Jocelyn Roth, Wendy L. Queen, Kalle S. Mertin, Danielle E. Schier, Neil R. Champness, Hamish H.-M. Yeung, and Bettina V. Lotsch**

Dedicated to the memory of Professor Peter Behrens

Metal–organic frameworks (MOFs) are a rapidly growing class of materials that offer great promise in various applications. However, the synthesis remains challenging: for example, a range of crystal structures can often be accessed from the same building blocks, which complicates the phase selectivity. Likewise, the high sensitivity to slight changes in synthesis conditions may cause reproducibility issues. This is crucial, as it hampers the research and commercialization of affected MOFs. Here, it presents the first-ever interlaboratory study of the synthetic reproducibility of two Zr–porphyrin MOFs, PCN-222 and PCN-224, to investigate the scope of this problem. For PCN-222, only one sample out of ten was phase pure and of the correct symmetry, while for PCN-224, three are phase pure, although none of these show the spatial linker order characteristic of PCN-224. Instead, these samples resemble dPCN-224 (disordered PCN-224), which has recently been reported. The variability in thermal behavior, defect content, and surface area of the synthesised samples are also studied. The results have important ramifications for field of metal–organic frameworks and their crystallization, by highlighting the synthetic challenges associated with a multi-variable synthesis space and flat energy landscapes characteristic of MOFs.

1. Introduction

Metal–organic frameworks (MOFs) show a large number of applications,[1,2] including catalysis,[3] drug delivery,[4] and sensing.[5] The versatile functionality stems from the rich diversity of MOF structures, enabled by the nearly infinite combinations of inorganic nodes and organic linkers used as the building blocks. A MOF is defined by its chemical composition and topology, where the latter shows the connectivity of the underlying net. The topology is dictated by the geometry and coordination numbers of the building blocks, but often several topologies are available for a specific composition. This leads to polymorphism; a particularly well-known example is the zeolitic imidazolate frameworks (ZIFs),[6] but polymorphism also occurs for numerous other MOFs.[7–10]

Polymorphism indicates a shallow structural energy landscape, which, while highly useful for crystal engineering may cause

H. L. B. Boström, S. Emmerling, F. Heck, C. Koschnick, B. V. Lotsch
Max Planck Institute for Solid State Research
Heisenbergstraße 1, D-70569 Stuttgart, Germany
E-mail: hanna.bostrom@mmk.su.se; b.lotsch@fkf.mpg.de

H. L. B. Boström
Present address: Department of Materials and Environmental Chemistry
Stockholm University
Stockholm SE-106 91, Sweden

The ORCID identification number(s) for the author(s) of this article can be found under https://doi.org/10.1002/adma.202304832

DOI: 10.1002/adma.202304832

A. J. Jones, M. J. Cliffe
School of Chemistry
University of Nottingham
University Park, Nottingham NG7 2RD, UK

R. Al Natour, M. Bonneau, V. Guillerm, O. Shekhah, M. Eddaoudi
King Abdullah University of Science and Technology (KAUST)
Division of Physical Sciences and Engineering
Advanced Membranes & Porous Materials Center (AMPM)
Functional Materials Design
Discovery & Development Research Group (FMD3)
Thuwal 23955-6900, Kingdom of Saudi Arabia

J. Lopez-Cabrelles, S. Furukawa
Institute for Integrated Cell-Material Sciences (WPI-iCeMS)
Kyoto University
Kyoto 606-8501, Japan

synthetic challenges. If the topology is not uniquely stipulated by the composition and the different phases are energetically similar, phase selectivity during synthesis becomes nontrivial. Since MOFs are typically made in solution, structures with different stoichiometries of the building blocks may also form during the reaction. Consequently, inseparable phase mixtures of distinct polymorphs with potentially different properties will be obtained. Apart from being a nuisance for synthetic chemists, this also hampers the patenting of synthetic methods and prevents industrial applications.

Zr–porphyrin MOFs, comprising $Zr_6(OH)_4O_4$ clusters and tetrakis(4-carboxyphenyl)porphyrin (TCPP) ligands, present a prime example of structurally versatile MOFs. At least six different structures are known,[11–17] which differ in topology, linker/cluster ratio, and $Zr_6(OH)_4O_4$ connectivity [**Figure 1**]. First, two six-coordinated cubic structures with different linker arrangements exist: the linkers in PCN-224 (topology **she**) show checkerboard-like order,[14] whereas dPCN-224 (**ftw**) features linker disorder (d = disordered).[18] dPCN-224 was originally believed to consist of cubic Zr_8 clusters and named PCN-221.[15] Second, PCN-225 (**sqc**, $I4_1/amd$),[] NU-902 (**scu**, *Cmmm*),[16] and PCN-222 (**csq**, $P6/mmm$)[11–13] contain eight-coordinated clusters. Finally, the 12-coordinated PCN-223 (**shp**)[17] represents the densest member of the family. An additional 12-coordinated cubic structure, MOF-525 (**ftw**), has been reported,[13] although this crystal structure has been questioned.[18] As the ratio of cluster and linkers varies between the structures, they are not true polymorphs, but the above discussion of polymorphism applies nonetheless.

The strong Zr–carboxylate bonds[20] and the multifunctionality of porphyrin lead to potential applications of Zr–porphyrin MOFs. To illustrate, PCN-222 can detect and separate Cu^{II} with high sensitivity and selectivity,[21] and photocatalytically generate hydrogen gas from formic acid.[22] Furthermore, the cubic PCN-224 has been exploited in the construction of a qubit array for quantum computing.[23] The many phases possible for these Zr–porphyrin MOFs is an asset, as they diversify the available structures and thereby properties.

Reproducible synthesis of phase-pure Zr–porphyrin MOFs is nontrivial,[24] as the phase selectivity is determined by a plethora of synthesis parameters, e.g., temperature, concentration, and modulator. The exploration of the resulting multidimensional synthesis landscape to isolate the contribution of each parameter is difficult. Many researchers have attempted to establish links between synthesis conditions and reaction outcome,[24–27] but the results are conflicting. PCN-223 was originally suggested to be a kinetic product relative to MOF-525;[17] but a mechanochemical study found that MOF-525 instead transforms into PCN-223 upon ball milling.[26] Likewise, very similar conditions (90 °C for 18 h in excess acetic acid) have been reported for the synthesis of both PCN-223 and MOF-525.[25] Regarding PCN-222/224, increased reaction times at 145 °C seemed to favor PCN-222 relative to PCN-224,[27] whereas the converse result was obtained at 120 °C.[28] These examples illustrate the striking lack of consensus among the research on these MOFs.

Zr–porphyrin MOFs also suffer from notoriously irreproducible syntheses, where ostensibly identical conditions result in different products on different occasions[18,24]—a problem also noted for other MOFs. For example, the original synthesis of the archetypical UiO family,[29] could not always be replicated by other research groups.[30,31] Such discrepancies presumably arise from small changes in the synthesis environment when carried out by different researchers—changes that may not be easily noticed, e.g., ambient humidity. As reproducibility is a cornerstone of science, this presents a key challenge in the MOF field.

An interesting means to study reproducibility issues is an interlaboratory study (round robin study), which compares results from experiments carried out independently by different researchers or instruments. Such information minimizes the risk of drawing inaccurate conclusions based on false comparisons, as the natural spread in results is identified.[32] Several intriguing interlaboratory studies can be found within the physical sciences,[32–37] covering topics such as surface areas of porous systems,[34] ionic conductivities in solid electrolytes,[32] or strain analysis in X-ray diffraction.[36,37] Albeit time- and labour-intensive, interlaboratory studies provide a unique insight

S. Furukawa
Department of Synthetic Chemistry and Biological Chemistry
Graduate School of Engineering
Kyoto University
Kyoto 615-8510, Japan

M. Romero-Angel, C. Martí-Gastaldo
Instituto de Ciencia Molecular (ICMol)
Universitat de València
Catedrático José Beltrán-2, Paterna 46980, Spain

M. Yan, A. J. Morris
Macromolecules innovation institute
Virginia Tech
Blacksburg, VA 24061, USA

A. J. Morris
Department of Chemistry
Virginia Tech
Blacksburg, VA 24061, USA

I. Romero-Muñiz, Y. Xiong, A. E. Platero-Prats
Departamento de Química Inorgánica
Facultad de Ciencias
Universidad Autónoma de Madrid
Madrid 28049, Spain

A. E. Platero-Prats
Condensed Matter Physics Center (IFIMAC)
Universidad Autónoma de Madrid
Madrid 28049, Spain

A. E. Platero-Prats
Institute for Advanced Research in Chemical Sciences (IAdChem)
Universidad Autónoma de Madrid
Madrid 28049, Spain

J. Roth, W. L. Queen
Institute of Chemical Sciences and Engineering
École Polytechnique Fédérale de Lausanne (EPFL)
Sion CH-1950, Switzerland

K. S. Mertin
Institute of Inorganic Chemistry
Christian-Albrechts-University Kiel
24118 Kiel, Germany

D. E. Schier, N. R. Champness, H. H.-M. Yeung
School of Chemistry
University of Birmingham
Edgbaston, Birmingham B15 2TT, UK

B. V. Lotsch
Department of Chemistry
University of Munich (LMU)
Butenandtstrasse 5-13, Haus D, 81377 Munich, Germany

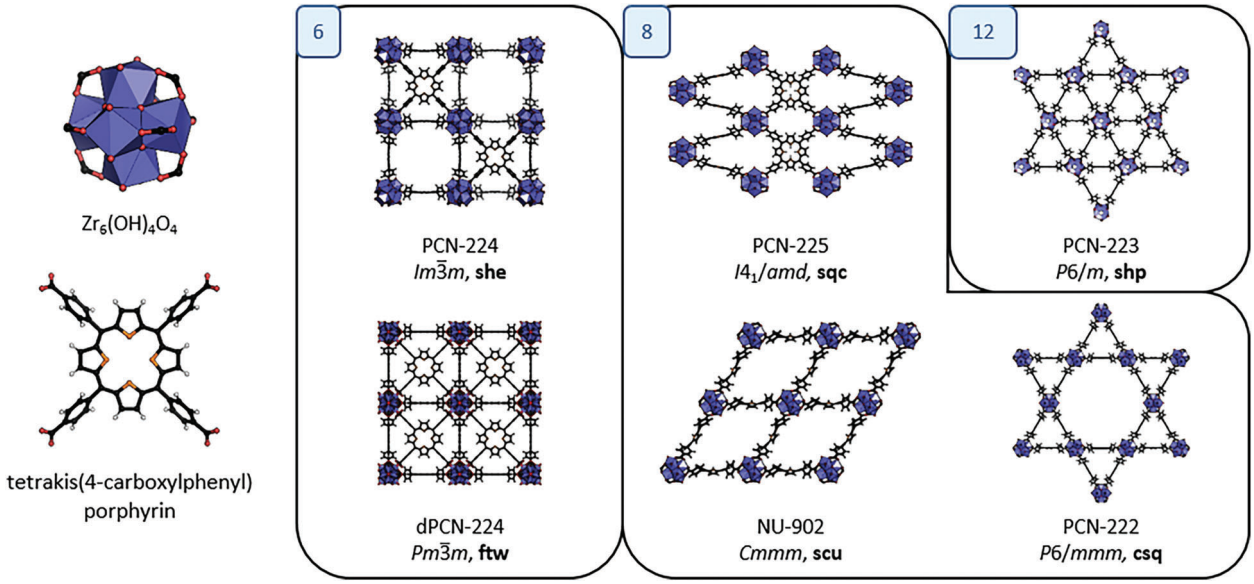

Figure 1. Structures ~~accessible~~ based on the $Zr_6(OH)_4O_4$ cluster and tetrakis(4-carboxyphenyl)porphyrin ligand, arranged by coordination number of the cluster (6, 8, or 12). The space group and topology are also given.

into the practical outcomes of experiments not obtainable by other means.

In this manuscript, we explore the synthetic reproducibility of the Zr–porphyrin MOFs PCN-222 and PCN-224 by performing the first-ever round robin study of MOF synthesis. The ten participating research groups independently targeted the two MOFs based on given experimental procedures from literature[11,14] and characterized the products by powder X-ray diffraction (XRD), scanning electron microscopy (SEM), thermogravimetric analysis (TGA), physisorption, and infrared (IR) spectroscopy. The synthetic outcome is highly variable: only 1–3 samples out of ten corresponds to the target phase, and the linker-disordered dPCN-224 was always obtained in lieu of the ordered PCN-224. A discussion considering possible reasons for the variation in results is given, and the article finishes with an outlook and some practical recommendations for synthetic MOF chemists. We stress that the objective of the study is not to test the validity of the original synthesis protocol, but rather to highlight the large variability in the obtained products.

2. Experimental Section

The ten participating groups received detailed instructions regarding the synthesis of PCN-222 and PCN-224 [ESI]. The syntheses were taken from literature,[11,14] but scaled up to ensure that sufficient amounts of material for the characterization were produced. The scaled-up reactions were attempted by the lead laboratory and pure samples were obtained, which confirms that the scale-up did not noticeably affect the feasibility of the synthesis. Briefly, the synthesis involved the combination of $ZrCl_4$ and metal-free tetrakis(4-carboxyphenyl)porphyrin in DEF (PCN-222) or DMF (PCN-224) with benzoic acid as a modulator. The reaction mixtures were heated at 120 °C for 48 h (PCN-222) or 24 h (PCN-224), and washed with DMF (3×6 ml) and acetone (3×6 ml).

Following synthesis, half of the sample material was sent to the lead laboratory. The products were characterized by X-ray diffraction (XRD), scanning electron microscopy (SEM), thermogravimetric analysis (TGA), and infrared (IR) spectroscopy by both the participating groups and at the lead laboratory [ESI]. Subsequently, activation using dilute HCl (100 °C, 24 h) was performed and the characterization suite was repeated, along with physisorption analysis [ESI]. Chemical activation had proved successful for the removal of modulators etc. from Zr-MOFs[38] and the procedure was taken from Ref. [39]. To facilitate comparisons, only the data collected at the lead laboratory are reported here. Every reasonable effort was made to minimize storage/transport times between synthesis and measurements and the samples were stored in inert atmospheres.

A note on nomenclature is in place here. The sample series synthesized from the procedure reported to give PCN-222 (PCN-224) is referred to as the PCN-222 (PCN-224) series, irrespective of whether the synthesis was successful. Individual samples were labeled with a letter (A–J) denoting the participating research group and a number (2 or 4) denoting PCN-22**2** or PCN-22**4**, respectively. For example, sample C4 was synthesised by group C using the procedure reported to yield PCN-224.

3. Results

Although the synthetic procedures originally yielded single crystals,[11,14] all participants obtained polycrystalline material with μm-sized particles [Figures S1– S4, Supporting Information]. As the reactions were scaled up, this may disfavor the formation of crystals. The sample colors varied from purple (e.g., F2 and F4), green (e.g., I2 and I4), or brown (e.g., D2 and D4). However, color descriptions can be subjective,[40] especially since the samples are very dark.

Typical yields, with TCPP as the limiting reagent, ranged from 60 to 160% for the two series [Table S2, Supporting Information]. Values over 100% highlight the need for careful drying and/or activation. Average yields following activation are ≈57% for PCN-222 and ≈77% for PCN-224 [Table S2, Supporting Information] and the relatively low values indicate that a large amount of material—e.g., solvent/unreacted materials is lost during activation and/or washing. In one case (I2), insufficient quantities of sample were obtained to allow for activation.

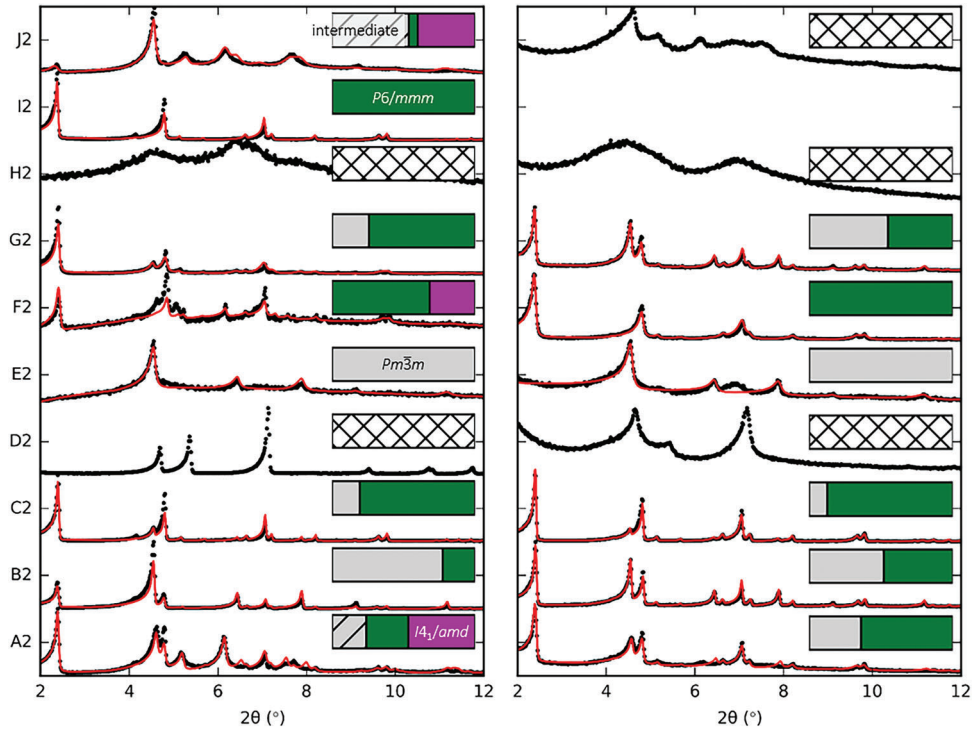

Figure 2. The XRD patterns of the ten samples from the PCN-222 series, with crude and activated MOFs to the left and right, respectively. The experimental data are shown in black with the calculated Rietveld fits in red and the inserted bar charts show the phase fractions obtained from the refinement. Color code: grey denotes $Pm\bar{3}m$ (dPCN-224), purple $I4_1/amd$ (PCN-225), and green $P6/mmm$ (PCN-222). Dashed grey bars denote a cubic-like intermediate and crossed white bars indicate samples that cannot be fitted by the aforementioned phases. The low sample quantity of I2 prevented activation. $\lambda = 1.5418$ Å.

3.1. The PCN-222 Series

The XRD patterns of the PCN-222 series and—for crystalline samples—the fit from Rietveld refinements[41] are shown in **Figure 2** and Figures S5–S7 (Supporting Information). The identity of the ten samples varies widely: the XRD pattern of PCN-222 is characterized by the intense 100 reflection ($2\theta \approx 2$ ° for Cu $K_{\alpha 1}$ radiation), and while this is present in most samples (A2, B2, C2, F2, G2, I2, and J2), its relative intensity varies drastically. This indicates phase mixtures, which is also supported by SEM [Figures S1– S2, Supporting Information]. PCN-222 appears as long rods with clear hexagonal symmetry, yet several morphologies—often cubes or similar—are typically observable as well. Three samples (D2, E2, H2) did not yield any PCN-222 product: H2 is largely amorphous, E2 corresponds to phase-pure dPCN-224 and D2 will be discussed below. The results showcase a surprisingly wide variety of outcomes from an identical synthetic recipe.

Rietveld refinements allow the phases present to be extracted and quantified [bars in Figure 2]. Caution is however required: The relatively poor quality of the laboratory XRD data and the multiple phases often render the fits challenging, particularly for less crystalline samples. The relative intensities of reflections can be heavily influenced by solvent and pore content, which also increases the uncertainty. Furthermore, the phase fractions do not account for any amorphous content and therefore only represent the crystalline part of the sample. The amorphous content was quantified for a few samples, and as an example, the amorphous phase fraction of activated A2 is ≈ 21% [Figure S11, Supporting Information]. However, this is a rough estimate, as quantifying amorphous contents is challenging. Despite these caveats, Figure 2 provides a useful approximation of the crystalline phase fractions of the ten samples.

Delving deeper into Figure 2, six samples are combinations of known Zr–porphyrin MOFs. E2 and I2 consist of pure dPCN-224 and PCN-222, respectively; B2, C2, and G2 are mixtures of these MOFs; and F2 can be fitted by a combination of PCN-222 and PCN-225 [Figure 2]. The remaining four compounds offer some surprises: A2 and J2 contain reflections characteristic of PCN-222 and PCN-225, but also a strong peak at ≈4.5°. This could normally be attributed to the cubic PCN-224, but the remaining reflections expected from this phase are absent. Such a diffraction pattern—denoted by a hashed grey bar in Figure 2—resembles that attributed to an intermediate phase ("phase II") in the formation of dPCN-224, consisting of $Zr_6(OH)_4O_4$ clusters with partial order.[28] D2 and H2 are discussed below.

Activation using HCl greatly affects the samples, in particular those featuring the presumed tetragonal PCN-225. Upon activation, this tetragonal phase vanishes completely from the three samples where it was present in the crude products (A2, F2, J2). The changes are particularly notable in F2, which corresponds to phase-pure PCN-222 following activation. Like most Zr–porphyrin systems, PCN-225 is known to be highly stable and should survive the harshly acidic environment found

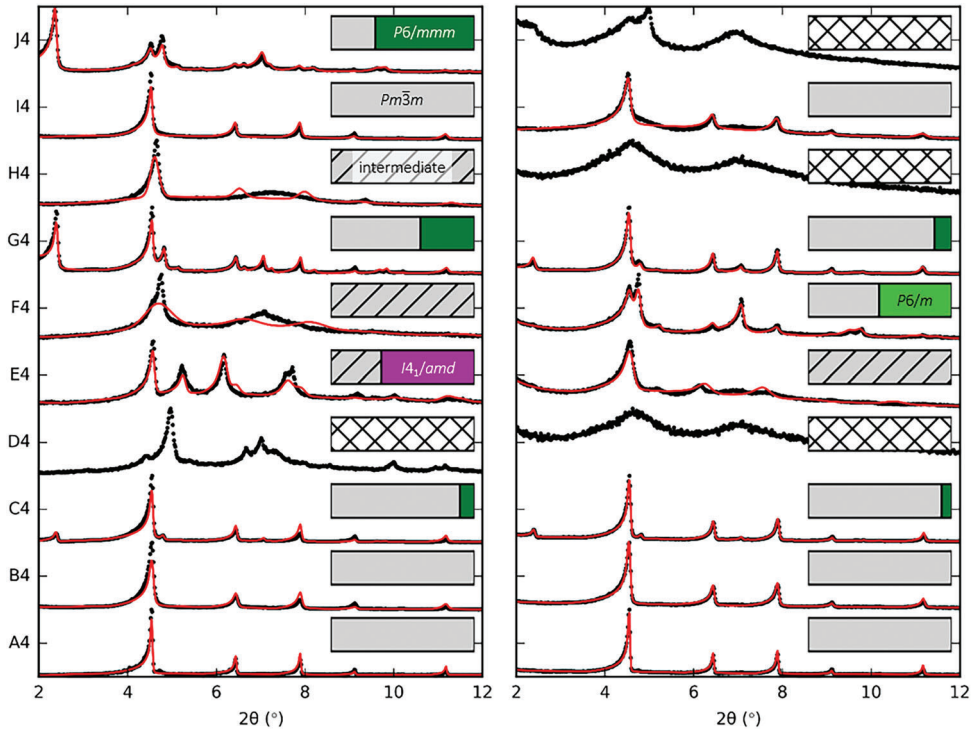

Figure 3. The XRD patterns of the ten samples from the PCN-224 series, with crude and activated MOFs to the left and right, respectively. The data are shown in black with Rietveld fits in red and the inserted bar charts show the phase fractions obtained from the refinement. Color code: grey denotes $Pm\bar{3}m$ (dPCN-224), purple $I4_1/amd$ (PCN-225), green $P6/mmm$ (PCN-222), light green $P6/m$ (PCN-223). Dashed grey bars denote a cubic-like intermediate and crossed white bars indicate samples that cannot be fitted by the aforementioned phases. $\lambda = 1.5418$ Å.

during activation.[42] Therefore the instability toward activation implies that reflections assigned as PCN-225 do not correspond to a known crystalline MOF, but rather an unknown intermediate product, which either transforms into crystalline PCN-222 or PCN-224 during the activation step or becomes X-ray amorphous. Alternatively, it cannot be excluded that PCN-225 particles—if smaller than the remaining phases—could have been lost during the washing following activation.

Activation typically improves quality of the Rietveld refinements for the crystalline samples, as removing unreacted starting material/solvent etc. from the pores enhances the similarity with the solvent-free crystal structures from literature. In addition, the phase fractions often change slightly after activation. While this may result from the loss of small particles during washing, the improvement of the fit due to solvent removal likely dominates and the phase fractions for the activated samples are thus more accurate. The average phase fraction of PCN-222 can be defined as $\frac{1}{10}\sum_i w_i^{222}$, where w_i^{222} is the weight percent of PCN-222 of sample i and the summation includes all ten samples. This value is 38% both before and after activation; note that any amorphous content is not accounted for. The SEM images show that although the surface of the particles appear more "etched" after the activation, the overall morphology is usually retained [Figures S1– S2, Supporting Information]. So in general, activation improves the purity of Zr–porphyrin MOFs.

The diffraction patterns belonging to D2 and H2 cannot be fitted using known Zr–porphyrin MOF phases, albeit for different reasons. Neither shows any clear morphology in the SEM images, but while H2 is amorphous, D2 has periodicity with sharp Bragg reflections. This XRD pattern can be fitted by an *I*-centred orthorhombic cell with lattice parameters ($a \approx 32.8$ Å, $b \approx 37.5$ Å, $c \approx 11.3$ Å). However, given that the porphyrin linkers span ≈16 Å, a 3D MOF with a periodicity of merely 11 Å along c is unlikely. In addition, the crystallinity was lost upon activation, which is unexpected for a 3D network joined by strong Zr–carboxylate bonds. Consequently, D2 is perhaps a molecular or metal–organic structure with low-dimensional order, rather than a 3D framework.

3.2. The PCN-224 Series

Similarly to the PCN-222 series, the PCN-224 series contains a variety of products (**Figure 3**; Figures S8 – S10, Supporting Information). Three samples (A4, B4, I4) consist of largely phase-pure dPCN-224 ($Pm\bar{3}m$), yet not a single sample corresponds to the targeted linker-ordered PCN-224 ($Im\bar{3}m$). The pattern of A4 contains an extremely weak reflection at ≈5°, presumably from a minor impurity phase (possibly PCN-225). While A4 and B4 feature cubic and cuboctahedral morphology, the particles of I4 show no clear facets [Figure S4, Supporting Information]. C4, G4, and J4 are mixtures of dPCN-224 and PCN-222—the latter easily identified by the 100 reflection at 2° and the rod-like morphology [Figures S3 and S4, Supporting Information]. The remaining four samples consist of low-crystalline products, including the intermediate "phase II" (E4, F4, H4) discussed above.[28] E4 also features reflections reminiscient of tetragonal PCN-225. Overall,

the products obtained from the PCN-224 synthesis are highly heterogeneous (Figure 3), although the spread is perhaps slightly lower than for the PCN-222 series.

PCN-224[14] and dPCN-224[18]—originally known as PCN-221[15]—share the same cubic symmetry but differ in the extent of spatial linker order. The superstructure of PCN-224 yields $Im\bar{3}m$ symmetry, whereas the average structure of the disordered dPCN-224 adopts the space group $Pm\bar{3}m$. Surprisingly, no sample in the PCN-224 series shows long-range linker order, although locally ordered domains with short correlation lengths cannot be excluded. The linker order originally observed in PCN-224 hence appears elusive and challenging to access synthetically. Local linker/vacancy order can have functional implications,[43,44] and hence further studies into the linker arrangement in dPCN-224/PCN-224 would be valuable.

Activation normally enhances the quality of the Rietveld fits for the crystalline samples, whereas poorly ordered samples often amorphize. For example, the Rietveld fit of B4 is noticeably improved following activation, whereas D4 loses its Bragg reflections. However, a few interesting counterexamples to this general trend exist. First, crude F4 only features a handful of diffraction peaks, yet can be well fitted by a combination of dPCN-224 and PCN-223 ($P6/m$) when activated. The converse scenario occurs for J4, which consists of PCN-222 and PCN-224 prior to activation, but is largely amorphous afterward, although the rod-like morphology characteristic of PCN-222 is retained [Figure S4, Supporting Information]. As mentioned, the PCN-225 phase in E4 vanishes after activation, suggesting that it might correspond to an intermediate. The average phase fraction of cubic Zr–porphyrin MOFs is ≈48% before activation and 53% after; however, the disordered dPCN-224 ($Pm\bar{3}m$) is exclusively obtained over the ordered PCN-224 ($Im\bar{3}m$). Hence, if dPCN-224 and PCN-224 are considered distinct phases, the success rate is 0%. Apart from the additional complications regarding the linker (dis)order, the results agree with the observations made for PCN-222.

A caveat regarding PCN-223—as seen in activated F4—is in order. PCN-223 crystallises in $P6/m$ with a disordered 12-fold coordinated $Zr_6(OH)_4O_4$ cluster located at a sixfold rotation axis.[17] However, a linker-disordered version of PCN-222 (**csq**) or a spatial average of different domains of NU-902 (**scu**) yield very similar diffraction patterns. Therefore, distinguishing between PCN-223 and NU-902 is difficult, and an equally good fit of activated F4 was obtained using NU-902 (Figure S12, Supporting Information). Caution should be observed when analyzing diffraction data for these phases.

The activated samples generally retained crystallinity for at least a few months following storage under argon. While systematic stability tests were beyond the scope of the study, the behavior of H4 is notable: the XRD pattern collected by Group H indicates substantially higher crystallinity than the pattern collected a few weeks later, following transport to the lead laboratory (Figure 3). This hints that stability might vary between individual MOFs, and long-term stability tests will be crucial for future applications.

The lattice parameters of the dPCN-224 and PCN-222 fractions vary slightly between different samples [Figure S13 and Tables S4 – S5, Supporting Information].[11,18] For cubic dPCN-224, a ranges from 19.28 to 19.36 Å, which lies within ±0.6% of the literature value.[18] A small shift (increase or decrease) typically occurs upon activation. PCN-222 shows a somewhat larger deviation of ±1.5% from the literature value.[11] Activation typically induces relatively large changes to both a and c of PCN-222, although the direction of change varies. However, expansion along a is always accompanied by contraction along c or vice versa. Given the flexible nature of MOFs and the guest dependence of lattice parameters,[45–48] the variations are unsurprising.

4. Discussion

The most striking feature of this study is the large variability in the identity of samples arising from identical given synthesis conditions. Thus, the reproducibility is very low. Apart from phase mixtures of known Zr–porphyrin MOFs, numerous unidentifiable products and low-crystalline powders were obtained. For PCN-222, only one of ten syntheses gave a phase-pure sample of the target compound, whereas three samples of nominally PCN-224 consist of phase-pure linker-disordered dPCN-224.[18] Despite the linker disorder, the higher success rate for PCN-224 indicates that the synthesis of the cubic phase is perhaps more robust. Both synthetic procedures occasionally gave a majority product of an alternative MOF (i.e., PCN-224 was formed when PCN-222 was targeted or vice versa). The synthetic conditions in favor of PCN-222 and PCN-224 are clearly sufficiently similar that fluctuations depending on human/environmental factors can direct the reaction toward the undesired phase. Other Zr–porphyrin MOFs were rarely observed, indicating that PCN-224/dPCN-224 and PCN-222 are the most favorable forms under these conditions.

The results prompt the question of what factors underpin the low reproducibility. The synthetic factors controlled here—solvent, modulator, temperature, time, and reagent concentration—are clearly insufficient to impart full control over phase selectivity. As seen in the SI, slight differences appear in e.g., the size of the reaction vial (20–50 ml), reagent purity, soaking time between washes (minutes–hours), drying time (overnight to over a weekend), and dissolution method (sonication or not). Ascertaining the influence of each of these changes requires further research, yet this demonstrates the large scope for variation offered by a standard synthetic recipe.

Variable water content is likely a partial cause of the difference in results. The kinetic effects of water on the formation of PCN-224/dPCN-224 were recently highlighted.[28] $ZrCl_4$ is hygroscopic; thus pristine $ZrCl_4$ results in an intermediate, whereas $ZrCl_4$ exposed to air yields either PCN-222 or PCN-224 depending on the exposure time.[28] While anecdotal, it is worth noting that D2 and D4, which were synthesised from anhydrous Zr, did not yield any known Zr–porphyrin MOF and amorphized upon activation. The importance of water is also known for other MOF syntheses.[49–52] In addition to the water in the Zr^{IV} source, ambient humidity, and the water content of the solvent will vary. The participants in this study span climates ranging from desert to humid subtropical,[53,54] which may have an effect—although many modern labs are air-conditioned. Likewise, the freshness of the solvent is critical, as amide-based solvents are prone to hydrolysis. Repeating the inter-laboratory study with water as a controlled variable would provide an estimate of the extent to which water dictates the synthetic outcome.

Besides water, other factors may also contribute to the variation in results. The reactions involve a significant build-up of

pressure, dictated by the volume and headspace of the reaction vessel, which were not controlled in our study. Our experiences indicate that changing the volume ratio of the reaction mixture relative to the vial can affect the phase selectivity of the product, presumably due to changes in pressure. Unintentional evaporation may also affect the concentration. Most participants used reaction vessels with volumes of 20–30 ml, but a 50 ml-vial was also used in one instance. Finally, the actual temperature of the reaction may vary depending on the heating source, temperature gradients, and calibration, and this could contribute to the deviation in results.

An intriguing concept sometimes invoked to explain discrepancies in synthesis is accidental seeding. If material from previous syntheses is present in the lab, this might act as crystallization seeds and direct the synthesis toward a particular polymorph. An extreme example occurs in so-called disappearing polymorphism,[55,56] where a synthesis reliably gives rise to a particular polymorph, but suddenly—upon the accidental introduction of seeds of a more stable form—fails to produce the initial polymorph in favor of the more stable one. This problem is well documented in pharmaceutical research, with Ritonavir being a high-profile example.[57] Seeding can influence the reaction outcomes of MOFs—and has indeed been suggested as a method of directing the synthesis[58]—and may also play a role in the reproducibility issues.

One potential weakness of our study is that the samples were sent to the lead laboratory for analysis and differences in storage times and shipping conditions could have had an impact. In most cases (B2-H2, B4-C4, E4-F4, I4-J4), the XRD patterns collected by the lead lab agree well with those collected by the participants immediately after the synthesis, albeit differences in resolution and signal strength are clear in some cases. This indicates that the samples did not change during the transport and justifies our approach. Some samples (J2 and G4) show differences in the intensity distributions between the two data collections. I2 presents an extreme example of this, where the low-angle peak characteristic of PCN-222 is absent in the data collected by the participating group. Given the small amounts of samples used and potentially different diffraction geometries, such changes could relate to preferred orientation, although sample recrystallization cannot be excluded. D4 is more crystalline after activation carried out by the participant compared to the lead laboratory, even though the crude samples were similar in both data collections. This indicates a sensitivity to the exact activation conditions. In general, the samples where phases can be clearly identified show a good agreement between the data collected by the group and by the lead lab.

Still, the XRD patterns of A2 and H4 exhibit large differences when collected by the participants and by the lead lab. The former shows severe changes to the intensity profile in its crude form and activation by the participant gave a different product compared to when carried out by the lead lab. The product obtained by the lead lab is at best a mixture of phases, whereas that obtained by the participant resembles PCN-224, but with a larger lattice parameter. The XRD pattern of H4 indicated larger crystallinity when measured by group H compared to when collected by the lead laboratory following transport. These samples had the longest storage time (several weeks) due to unforeseen circumstances and decomposition is the most likely explanation. These

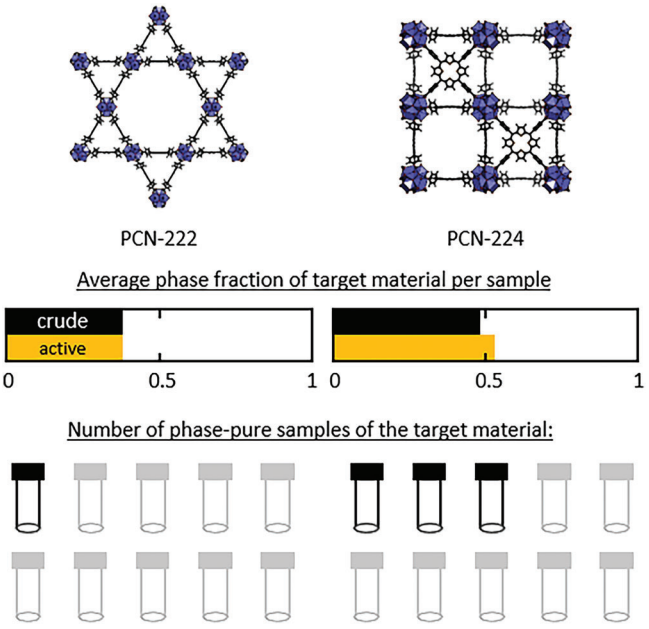

Figure 4. The main results of the study, including the average phase fraction of target material per sample for crude (black) and activated (orange) samples, and the number of phase-pure samples obtained of the target MOF out of the ten synthesized samples: one for PCN-222 and three for PCN-224. The disordered dPCN-224 is treated as equivalent to the linker-ordered PCN-224. The results only consider the crystalline part of the samples.

results call for further stability tests of the compounds and also highlight the limitations of our study. Further studies on the long-term stability in different chemical environments will be useful for both fundamental and applied researchers.

This study also raises questions about the post-synthetic HCl activation of MOFs. While thermal activation or supercritical CO_2-drying may be more common methods for removing pore content,[38,59] the use of dilute HCl is necessary for the removal of coordinated modulators.[38] The changes to the XRD patterns following activation can be explained by the removal of pore content or the decomposition of unstable intermediates. This can aid the distinction of crystalline MOFs from intermediates with partial crystallinity, as the latter are less stable toward activation. Less rationalisable changes are observed in the TGA traces after activation [ESI], where the decomposition becomes more gradual and shifts to lower temperatures. Speculatively, this could indicate changes to the coordination or the bonding—as the cluster–linker bonds are presumably the weakest link—and an increased spread of local environments. This would mean that the framework collapse of MOFs with pore content is delayed until the pores are empty, whereas they are already empty in the activated MOFs, thus the onset of pore collapse occurs earlier. While some studies on the chemical changes induced by activation exist,[60] further exploration of the effect of activation—particularly using local probes—would be illuminating.

Closely related to activation is the challenge of characterizing defects in Zr–porphyrin MOFs. Like for the UiO family,[61,62] defects in the form of deviations from the ideal stoichiometry are known in Zr–porphyrin systems.[18,24] TGA gives an indirect

measure of the linker/cluster ratio and hence the fraction of missing linkers, although the precision of TGA varies.[63] However, this assumes that missing linkers are the only type of defect present, which may not be true. Missing-cluster defects[61] have been suggested to be the dominant type of defects in archetypical UiO-66, and can be detected by XRD by virtue of their (partial) order.[62] Conversely, disordered cluster vacancies are difficult to observe, but the high linker/cluster ratio found by TGA for some samples here may point towards such defects. Likewise, the linker/cluster ratio occasionally increases following activation, which could imply the removal of Zr^{IV}—alone or as part of a cluster. This motivates future studies into the role of activation and defectivity.

Finally, it is worth speculating about the compositional factors of a particular MOF system that are conducive to unreliable synthetic outcomes. The cluster coordination preference is clearly key: the $Zr_6(OH)_4O_4$ cluster can vary its coordination from 4 to 12, leading to a wealth of available topologies. Orientational order of the cluster, and the ability to support various binding modes of the linker[18] may also play a role. The linker is also relevant, as MOFs based on $Zr_6(OH)_4O_4$ and tetrakis(4-carboxyphenyl)pyrene ligands only form **scu** and **csq** topologies.[64,65] This could be due to the lower symmetry of pyrene relative to porphyrin, preventing the formation of cubic topologies. Hence, the synthetic reliability of a particular MOF system is influenced by topological factors, but chemistry and preference of the building blocks may also be implicated.

5. Conclusion

The key message of this study is that reproducible MOF synthesis can be tremendously challenging. The number of phase-pure samples ranges from 1 to 3 (if dPCN-224 is considered a success when PCN-224 is targeted) [**Figure 4**] and the average phase fraction of the target phase is 50% at most. Since the separation of related phases is challenging, the phase mixtures would be unsuitable for most practical purposes. While we have focused on the difference between syntheses carried out in different labs, irreproducibility issues within the same lab are also noted. So although the flat structural energy landscape of MOFs is beneficial—by allowing access to a large number of structures and properties—the downside can be synthetic difficulties.[66] Yet, if synthetic control can be obtained, precise tuning of e.g., pore shape will be enabled. Consequently, while establishing reproducible links between synthesis and topology of Zr–porphyrin MOFs will undoubtedly require a large amount of work—and has indeed been started[24–26]—the reward will be substantial.

Our results lead to a set of recommendations for MOF chemists. First, reports of new MOF structures should include detailed experimental details, as many factors influence the outcome—including parameters typically not mentioned. For instance, the water content of the solvent and precursors, the ambient humidity, or the size of the reaction vessel can be critical to success and often vary between different labs. Second, one could investigate the reproducibility of newly synthesized compounds, e.g., by reporting the outcomes from at least two independent syntheses carried out by two (or more) researchers. While this increases the workload, it would help validate the results and the experimental procedures. Even if only one researcher succeeds in producing the target compound, this does not invalidate the new structure, but simply highlights the sensitive nature of the synthesis. Thus, a greater extent of openness in the reporting of synthesis would be tremendously beneficial.

Third, further investigations into the link between synthetic parameters and reaction outcomes are required, and also into the formation mechanisms of MOFs. As the set of synthetic parameters forms a large multi-dimensional space, high-throughput and automated synthesis approaches assisted by machine-learning/AI will be useful.[25] Ultimately, irreproducibility issues are underpinned by poor understanding of the MOF formation mechanisms. These are complex processes depending (at least partially) on the system and conditions, and require multi-technique approaches capable of probing different time- and length scales.[67] While many excellent in situ studies of MOF crystallization processes exist,[68–74] these are still relatively few compared to the vast number of known MOFs. Moreover, computational studies to model reaction mechanisms or calculate relative energies of competing phases will be valuable.

Finally, while reproducibility is a cornerstone of the scientific method, irreproducibility in MOF synthesis does not necessarily equate to poorly conducted research. Irreproducible syntheses simply indicate that the reaction is sensitive to yet unknown factors and the—possibly very challenging—task is to identify and control these factors. Likewise, this study does not question the synthetic protocols[11,14] employed here. Needless to say, irreproducibility is a nuisance and in light of this, a database of verified syntheses has been proposed.[75] In addition, AI-assisted, automated synthesis could be a game changer in making synthesis processes more robust and reproducible. This could not only save time, but also shed light on factors conducive to synthetic reproducibility. Yet, further insight into MOF synthesis is still required to fully enable the potential of this promising class of materials to be realized.

Supporting Information

Supporting Information is available from the Wiley Online Library or from the author.

Acknowledgements

HLBB acknowledges financial support from the Alexander von Humboldt Foundation. V. Duppel (MPI-FKF) is gratefully acknowledged for collecting the SEM images and S. Krause (MPI-FKF) and N. Stock (Kiel) for useful discussions. MJC acknowledges the School of Chemistry, University of Nottingham, for support from the Hobday bequest. AJJ acknowledges funding provided by the EPSRC under grant number: EPSRC/SFI CDT in Sustainable Chemistry – Atoms 2 Products (EP/S022236/1). RN, MB, VG, OS, and ME acknowledge the support of the King Abdullah University of Science and Technology (KAUST). CMG and MRA acknowledge FPI Scholarships PRE2018-083327 and MCIN/AEI/10.13039/501100011033 (projects PID2020-118117RB-I00 & EUR2021-121999) for funding. Virginia Tech Nanoscale Characterization and Fabrication Laboratory were used for SEM and X. Yang, H. Cornell, M. J. Bortner, and Y. Yao are thanked for assistance with analysis. The NCFL facilities were supported by NanoEarth and National Nanotechnology Coordinated Infrastructure who were funded by ECCS 1542100 and ECCS 2025151. This work was supported by PID2021-123839OB-I00 and EUR2020-112294 funded by MCIN/AEI/10.13039/501100011033 and by

the European Union "NextGenerationEU"/PRTR. A.E.P.-P. acknowledges the financial support from the Spanish Ministry of Science and Innovation through the "María de Maeztu" Programme for Units of Excellence in R&D 445 (CEX2018-000805-M). A.E.P.-P. acknowledges the Spanish Ministry of Science and Innovation for a Ramón y Cajal fellowship (RYC2018-024328-I). I.R.-M. acknowledges FPI-UAM 2019 fellowship from UAM. . HHMY acknowledges the EPSRC grant EP/W010151/1, "Unlocking the pre-nucleation state as a route to materials discovery in MOFs". NRC gratefully acknowledged the support of the EPSRC (EP/S002995/2).

Open access funding enabled and organized by Projekt DEAL.

Conflict of Interest

The authors declare no conflict of interest.

Data Availability Statement

The data that support the findings of this study are available from the corresponding author upon reasonable request.

Keywords

metal–organic frameworks, reproducibility, synthesis

Received: May 22, 2023
Revised: August 17, 2023
Published online:

[1] R. Ricco, C. Pfeiffer, K. Sumida, C. J. Sumby, P. Falcaro, S. Furukawa, N. R. Champness, C. J. Doonan, *CrystEngComm* **2016**, *18*, 6532.
[2] R. Freund, O. Zaremba, G. Arnauts, R. Ameloot, G. Skorupskii, M. Dincă, A. Bavykina, J. Gascon, A. Ejsmont, J. Goscianska, M. Kalmutzki, U. Lächelt, E. Ploetz, C. S. Diercks, S. Wuttke, *Angew. Chem. Int. Ed.* **2021**, *60*, 23975.
[3] A. Dhakshinamoorthy, Z. Li, H. Garcia, *Chem. Soc. Rev.* **2018**, *47*, 8134.
[4] P. Horcajada, C. Serre, G. Maurin, N. A. Ramsahye, F. Balas, M. Vallet-Regí, M. Sebban, F. Taulelle, G. Férey, *J. Am. Chem. Soc.* **2008**, *130*, 6774.
[5] A. Karmakar, P. Samanta, A. V. Desai, S. K. Ghosh, *Acc. Chem. Res.* **2017**, *50*, 2457.
[6] K. S. Park, Z. Ni, A. P. Côté, J. Y. Choi, R. Huang, F. J. Uribe-Romo, H. K. Chae, M. O'Keeffe, O. M. Yaghi, *Proc. Natl. Acad. Sci. U.S.A* **2006**, *103*, 10186.
[7] P. K. Verma, L. Huelsenbeck, A. W. Nichols, T. Islamoglu, H. Heinrich, C. W. Machan, G. Giri, *Chem. Mater.* **2020**, *32*, 10556.
[8] V. Bon, I. Senkovska, I. A. Baburin, S. Kaskel, *Cryst. Growth Des.* **2013**, *13*, 1231.
[9] Z.-J.-. Li, Y. Ju, Z. Zhang, H. Lu, Y. Li, N. Zhang, X.-L.. Du, X. Guo, Z.-H. Zhang, Y. Qian, M.-Y. He, J.-.Q. Wang, J. Lin, *Chem. Eur. J.* **2021**, *27*, 17586.
[10] K. Barthelet, J. Marrot, G. Férey, D. Riou, *Chem. Commun.* **2004**, 520.
[11] D. Feng, Z.-Y. Gu, J.-R. Li, H.-L. Jiang, Z. Wei, H.-C. Zhou, *Angew. Chem. Int. Ed.* **2012**, *51*, 10307.
[12] Y. Chen, T. Hoang, S. Ma, *Inorg. Chem.* **2012**, *51*, 12600.
[13] W. Morris, B. Volosskiy, S. Demir, F. Gándara, P. L. McGrier, H. Furukawa, D. Cascio, J. F. Stoddart, O. M. Yaghi, *Inorg. Chem.* **2012**, *51*, 6443.
[14] D. Feng, W.-C. Chun, Z. Wei, Z.-Y. Gu, H.-L. Jiang, Y.-P. Chen, D. J. Darensbourg, H.-C. Zhou, *J. Am. Chem. Soc.* **2013**, *135*, 17105.
[15] D. Feng, H.-L. Jiang, Y.-P. Chen, Z.-Y. Gu, Z. Wei, H.-C. Zhou, *Inorg. Chem.* **2013**, *52*, 12661.
[16] P. Deria, D. A. Gómez-Gualdrón, I. Hod, R. Q. Snurr, J. T. Hupp, O. K. Farha, *J. Am. Chem. Soc.* **2016**, *138*, 14449.
[17] D. Feng, Z.-Y. Gu, Y.-P. Chen, J. Park, Z. Wei, Y. Sun, M. Bosch, S. Yuan, H.-C. Zhou, *J. Am. Chem. Soc.* **2014**, *136*, 17714.
[18] C. Koschnick, R. Stäglich, T. Scholz, M. W. Terban, A. von Mankowski, G. Savasci, F. Binder, A. Schökel, M. Etter, J. Nuss, R. Siegel, L. S. Germann, C. Ochsenfeld, R. E. Dinnebier, J. Senker, B. V. Lotsch, *Nat. Commun.* **2021**, *12*, 3099.
[19] H.-L.. Jiang, D. Feng, K. Wang, *J. Am. Chem. Soc.* **2013**, *135*, 13934.
[20] Y. Bai, Y. Dou, L.-H. Xie, W. Rutledge, J.-R. Li, H.-C. Zhou, *Chem. Soc. Rev.* **2016**, *45*, 2327.
[21] Y.-Z. Chen, H.-L. Jiang, *Chem. Mater.* **2016**, *28*, 6698.
[22] Y. Wang, X. Wang, H. Lu, Z. Gu, L. Chen, *Chem. Commun.* **2022**, *58*, 8520.
[23] C.-J. Yu, M. D. Krzyaniak, M. S. Fataftah, M. R. Wasielewski, D. E. Freedman, *Chem. Sci.* **2019**, *10*, 1702.
[24] S. M. Shaikh, P. M. Usov, J. Zhu, M. Cai, J. Alatis, A. J. Morris, *Inorg. Chem.* **2019**, *58*, 5145.
[25] M. L. Kelty, W. Morris, A. T. Gallagher, J. S. Anderson, K. A. Brown, C. A. Mirkin, T. D. Harris, *Chem. Commun.* **2016**, *52*, 7854.
[26] B. Karadeniz, D. Žilić, I. Huskić, L. S. Germann, A. M. Fidelli, S. Muratović, I. Lončarić, M. Etter, R. E. Dinnebier, D. Barišić, N. Cindro, T. Islamoglu, O. K. Farha, T. Friščić, K. Užarević, *J. Am. Chem. Soc.* **2019**, *141*, 19214.
[27] X. Gong, H. Noh, N. C. Gianneschi, O. K. Farha, *J. Am. Chem. Soc.* **2019**, *141*, 6146.
[28] C. Koschnick, M. T. Terban, S. Canossa, M. Etter, R. E. Dinnebier, B. V. Lotsch, *Adv. Mater.* **2023**, 2210613.
[29] J. H. Cavka, S. Jakobsen, U. Olsbye, N. Guillou, C. Lamberti, S. Bordiga, K. P. Lillerud, *J. Am. Chem. Soc.* **2008**, *130*, 13850.
[30] G. Wißmann, A. Schaate, S. Lilienthal, I. Bremer, A. M. Schneider, P. Behrens, *Microporous Mesoporous Mater.* **2012**, *152*, 64.
[31] A. Schaate, P. Roy, A. Godt, J. Lippke, F. Waltz, M. Wiebcke, P. Behrens, *Chem. Eur. J.* **2011**, *17*, 6643.
[32] S. Ohno, T. Bergnes, J. Buchheim, M. Duchardt, A.-K. Hatz, M. A. Kraft, H. Kwak, A. L. Santhosha, Z. Liu, N. Minafra, F. Tsuji, A. Sakuda, R. Schlem, S. Xiong, Z. Zhang, P. Adelhelm, H. Chen, A. Hayashi, Y. S. Jung, B. V. Lotsch, B. Roling, N. M. Vargas-Barbosa, W. G. Zeier, *ACS Energy Lett.* **2020**, *5*, 910.
[33] R. E. H. Kuveke, L. Barwise, Y. van Ingen, K. Vashisth, N. J. Roberts, S. S. Chitnis, J. L. Dutton, C. D. Martin, R. L. Melen, *ACS Cent. Sci.* **2022**, *8*, 855.
[34] J. W. M. Osterrieth, J. Rampersad, D. Madden, N. Rampal, L. Skoric, B. Connolly, M. D. Allendorf, V. Stavila, J. L. Snider, R. Ameloot, J. Marreiros, C. Ania, D. Azevedo, E. Vilarrasa-Garcia, B. F. Santos, X.-H. Bu, Z. Chang, H. Bunzen, N. R. Champness, S. L. Griffin, B. Chen, R.-B. Lin, B. Coasne, S. Cohen, J. C. Moreton, Y. J. Colón, L. Chen, R. Clowes, F.-X. Coudert, Y. Cui, et al., *Adv. Mater.* **2022**, *34*, 2201502.
[35] J. Rieger, *J. Therm. Anal.* **1996**, *46*, 965.
[36] D. Balzar, N. Audebrand, M. R. Daymond, A. Fitch, A. Hewat, J. I. Langford, A. Le Bail, D. Louër, O. Masson, C. N. McCowan, N. C. Popa, P. W. Stephens, B. H. Toby, *J. Appl. Cryst.* **2004**, *37*, 911.
[37] P. Colombi, D. K. Agnihotri, V. E. Asadchikov, E. Bontempi, D. K. Bowen, C. H. Chang, L. E. Depero, M. Farnworth, T. Fujimoto, A. Gibaud, M. Jergel, M. Krumrey, T. A. Lafford, A. Lamperti, T. Ma, R. J. Matyi, M. Meduna, S. Milita, K. Sakurai, L. Shabel'nikov, A. Ulyanenkov, A. van der Lee, C. Wiemer, *J. Appl. Cryst.* **2008**, *41*, 143.
[38] X. Zhang, Z. Chen, X. Liu, S. L. Hanna, X. Wang, R. Teheri-Ledari, A. Maleki, P. Li, O. K. Farha, *Chem. Soc. Rev.* **2020**, *49*, 7406.
[39] P. Deria, J. Yu, R. P. Balaraman, J. Mashni, S. N. White, *Chem. Commun.* **2016**, *52*, 13031.
[40] K. M. Jablonka, S. M. Moosavi, M. Asgari, C. Ireland, L. Patiny, B. Smit, *Chem. Sci.* **2021**, *12*, 3587.

[41] H. M. Rietveld, *Acta Crystallogr.* **1967**, *22*, 151.
[42] H.-L. Jiang, D. Feng, K. Wang, Z. Y. Guo, Z. Wei, Y.-P. Chen, H.-C. Zhou, *J. Am. Chem. Soc.* **2013**, *135*, 13934.
[43] A. Simonov, T. De Baerdemaeker, H. L. B. Boström, M. L. Ríos Gómez, H. J. Gray, D. Chernyshov, A. Bosak, H.-B. Bürgi, A. L. Goodwin, *Nature* **2020**, *578*, 256.
[44] S. M. J. Rogge, J. Wieme, L. Vanduyfhuys, S. Vandenbrande, G. Maurin, T. Verstraelen, M. Waroquier, V. Van Speybroeck, *Chem. Mater.* **2016**, *28*, 5721.
[45] E. J. Carrington, C. A. McAnally, A. J. Fletcher, S. P. Thompson, M. Warren, L. Brammer, *Nat. Chem.* **2017**, *9*, 882.
[46] A. Schneemann, V. Bon, I. Schwedler, I. Senkovska, S. Kaskel, R. A. Fischer, *Chem. Soc. Rev.* **2014**, *43*, 6062.
[47] C. Serre, F. Millange, C. Thouvenot, M. Noguès, G. Marsolier, D. Louër, G. Férey, *J. Am. Chem. Soc.* **2002**, *124*, 13519.
[48] H. L. B. Boström, S. Bette, S. T. Emmerling, M. W. Terban, B. V. Lotsch, *APL Mater.* **2022**, *10*, 071106.
[49] V. V. Butova, A. P. Budnyk, K. M. Charykov, K. S. Vetlitsyna-Novikova, C. Lamberti, A. V. Soldatov, *Chem. Commun.* **2019**, *55*, 901.
[50] F. C. N. Firth, M. J. Cliffe, D. Vulpe, M. Aragones-Anglada, P. Z. Moghadam, D. Fairen-Jimenez, B. Slater, C. P. Grey, *J. Mater. Chem. A* **2019**, *7*, 7459.
[51] M. Savić Biserčić, B. Marjanovic, B. Nedić Vasiljević, S. Mentus, B. A. Zasońska, G. Ćirić-Marjanović, *Microporous Mesoporous Mater.* **2019**, *278*, 23.
[52] F. Ragon, P. Horcajada, H. Chevreau, Y. K. Hwang, U.-H. Lee, S. R. Miller, T. Devic, J.-S. Chang, C. Serre, *Inorg. Chem.* **2014**, *53*, 2491.
[53] W. Köppen, *Meteorol. Z.* **1884**, *1*, 215.
[54] H. E. Beck, N. E. Zimmerman, T. R. McVicar, N. Vergopolan, A. Berg, E. F. Wood, *Sci. Data* **2018**, *5*, 180214.
[55] J. D. Dunitz, J. Bernstein, *Acc. Chem. Res.* **1995**, *28*, 193.
[56] D.-K. Bučar, R. W. Lancaster, J. Bernstein, *Angew. Chem. Int. Ed.* **2015**, *54*, 6972.
[57] J. Bauer, S. Spanton, R. Henry, J. Quick, W. Dziki, W. Porter, J. Morris, *Pharm. Res.* **2001**, *18*, 859.
[58] W.-J. Xu, K.-P. Xie, Z.-F. Xiao, W.-X. Zhang, X.-M. Chen, *Cryst. Growth Des.* **2016**, *16*, 7212.
[59] A. J. Howarth, A. W. Peters, N. A. Vermeulen, T. C. Wang, J. T. Hupp, O. K. Farha, *Chem. Mater.* **2017**, *29*, 26.
[60] Z. Lu, J. Liu, X. Zhang, Y. Liao, R. Wang, K. Zhang, J. Lyu, O. K. Farha, J. T. Hupp, *J. Am. Chem. Soc.* **2020**, *142*, 21110.
[61] M. J. Cliffe, J. A. Hill, C. A. Murray, F.-X. Coudert, A. L. Goodwin, *Phys. Chem. Chem. Phys.* **2015**, *17*, 11586.
[62] M. Taddei, *Coord. Chem. Rev.* **2017**, *343*, 1.
[63] B. Gibbons, E. C. Bartlett, M. Cai, X. Yang, E. M. Johnson, A. J. Morris, *Inorg. Chem.* **2021**, *60*, 16378.
[64] J. E. Mondloch, W. Bury, D. Fairen-Jimenez, S. Kwon, E. J. DeMarco, M. H. Weston, A. A. Sarjeant, S. T. Nguyen, P. C. Stair, R. Q. Snurr, O. K. Farha, J. T. Hupp, *J. Am. Chem. Soc.* **2013**, *135*, 10294.
[65] C.-W. Kung, T. Chiaan Wang, J. E. Mondloch, D. Fairen-Jimenez, D. M. Gardner, W. Bury, J. M. Klingsporn, J. C. Barnes, R. Van Duyne, J. F. Stoddart, M. R. Wasielewski, O. K. Farha, J. T. Hupp, *Chem. Mater.* **2013**, *25*, 5012.
[66] A. K. Cheetham, G. Kieslich, H. H.-M. Yeung, *Acc. Chem. Res.* **2018**, *51*, 659.
[67] D. J. Cerasale, D. C. Ward, T. L. Easun, *Nat. Rev. Chem.* **2022**, *6*, 9.
[68] F. C. N. Firth, M. W. Gaultois, Y. Wu, J. M. Stratford, D. S. Keeble, C. P. Grey, M. J. Cliffe, *J. Am. Chem. Soc.* **2021**, *143*, 19668.
[69] G. Zahn, P. Zerner, J. Lippke, F. L. Kempf, S. Lilienthal, C. A. Schröder, A. M. Schneider, P. Behrens, *CrystEngComm* **2014**, *16*, 9198.
[70] H. Xu, S. Sommer, N. L. Nyborg Broge, J. Gao, B. Brummerstedt Iversen, *Chem. Eur. J.* **2019**, *25*, 2051.
[71] H. H.-M. Yeung, A. F. Sapnik, F. Massingberg-Mundy, M. W. Gaultois, Y. Wu, D. A. X. Fraser, S. Henke, R. Pallach, N. Heidenreich, O. V. Magdysyuk, N. T. Vo, A. L. Goodwin, *Angew. Chem. Int. Ed.* **2019**, *58*, 566.
[72] F. Millange, M. I. Medina, N. Guillou, G. Férey, K. M. Golden, R. I. Walton, *Angew. Chem. Int. Ed.* **2010**, *49*, 763.
[73] M. Krüger, A. Ken Inge, H. Reinsch, Y.-H. Li, M. Wahiduzzaman, C.-H. Lin, S.-L. Wang, G. Maurin, N. Stock, *Inorg. Chem.* **2017**, *56*, 5851.
[74] M. J. Van Vleet, T. Weng, X. Li, J. R. Schmidt, *Chem. Rev.* **2018**, *118*, 3681.
[75] H. Reinsch, N. Stock, *Dalton Trans.* **2017**, *46*, 8339.